Effect of Coulomb screening length on nuclear "pasta" simulations

P. N. Alcain, P. A. Giménez Molinelli, J. I. Nichols, and C. O. Dorso
Departamento de Física FCEyN, UBA and IFIBA, Conicet, Pabellón 1, Ciudad Universitaria, 1428 Buenos Aires, Argentina
(Received 26 November 2013; revised manuscript received 12 February 2014; published 7 May 2014)

We study the role of the effective Coulomb interaction strength and length on the dynamics of nucleons in conditions according to those in a neutron star's crust. Calculations were made with a semiclassical molecular dynamics model, studying isospin symmetric matter at subsaturation densities and low temperatures. The electrostatic interaction between protons is included as a screened Coulomb potential in the spirit of the Thomas–Fermi approximation, but the screening length is artificially varied to explore its effect on the formation of the nonhomogeneous nuclear structures known as "nuclear pasta." As the screening length increases, we can see a transition from a one-per-cell pasta regime (due exclusively to finite-size effects) to a more appealing multiple pasta per simulation box. This qualitative difference in the structure of neutron star matter at low temperatures shows that special caution should be taken when the screening length is estimated for numerical simulations.

DOI: 10.1103/PhysRevC.89.055801 PACS number(s): 24.10.Lx, 02.70.Ns, 26.60.Gj, 21.30.Fe

I. INTRODUCTION

At densities and temperatures expected to exist in neutron star crusts ($\rho \lesssim \rho_0$ and $T \lesssim 1.0$ MeV, with ρ_0 denoting the normal nuclear density), nucleons form structures that are substantially different from the "normal," quasispherical nuclei we are familiar with. Such structures, which have been dubbed "nuclear pasta," have been investigated using various models [1–12] which have shown them to be the result of the interplay between nuclear and Coulomb forces in an infinite medium. The structure of the nuclear pasta is expected to play an important role in the study of neutrino opacity in neutron stars [13], neutron star quakes, and pulsar glitches [14]. In neutron stars, apart from protons and neutrons, there is an all-embedding electron gas. This electron gas screens the electrostatic long-range proton-proton interaction. This screening effect is often modeled within the Thomas–Fermi approximation, according to which the interaction between protons is a Yukawa-like potential with a screening length λ:

$$V_{TF}(r) = q^2 \frac{e^{-r/\lambda}}{r}.$$

According to quantum field theory calculations [15], pp. 175–180, the screening length at the densities of interest is $\lambda \approx 100$ fm. For numerical simulations, such a long-range interaction poses a problem since, to perform correct particle-based simulations, the simulation domain (or cell) should be much larger than the length of the interaction potentials [16]. Using the correct value for λ would then require working with $O(10^6)$ particles and it would be computationally very exhaustive. Facing this issue, pioneering authors [13,17] decided to work with a much smaller $\lambda = 10$ fm, hoping to retain the main qualitative phenomenological aspects of the system (competing interactions of different length) when dealing with smaller systems. Even if they were indeed capable of producing "pasta-like" structures, the particular choice of the value for the screening length was arbitrary and based almost solely on computational details. Notably, this particular value of the screening length was used by every author using a screened Coulomb potential for particle-based simulations ever since [7,12,13]. This paper will focus on studying to which extent this arbitrary choice is physically relevant, expanding previous works.

The role of the length of the screening has been narrowly explored by several authors in other models. For example, in a 2003 investigation [11], the screening effect of an electron gas on cold nuclear structures was investigated using a static liquid-drop model, and it was found that main effect of the gas screening was to extend the range of densities where bubbles and clusters appear and to reduce the range of stability of homogeneous phases. While the screening was found to be of minor importance, the study, being static, did not include any spatial or dynamical effect. Another 2005 study [18] used a density functional method to investigate charge screening on nuclear structures at subnuclear densities but still at zero temperature; in particular, cases with and without screening were directly compared. The main results of the study were nucleon density profiles used to quantify the spatial rearrangement of the proton- and electron-charge densities. Once again, it was found that the density region in which the pasta exists becomes broader when Coulomb screening is taken into account, mainly due to the rearrangement of the protons; the authors remark the importance of extending such a study to finite temperatures and with dynamical models. It was also observed [19], regarding the screening effect, that a very short screening length would mean a non-negligible coupling between protons and electrons. Under such conditions, the electrons would not be uniformly distributed and any eventual energy calculations neglecting the extra energy due to the electrons nonuniformity would be wrong. This, however, is far beyond the scope of this work.

More recently, some works [20,21] began studying the effect that Coulomb interaction has on the pasta formation by using dynamical models. The main findings are that artificial one-per-cell pasta (*pseudopasta*) could exist even when the Coulomb interaction was absent, and that they exist due to periodic boundary conditions and finite size [22].

In previous studies, it has been shown that a combination of molecular dynamics, fragment recognition algorithms, and a set of topological tools [10,12,23,24] was very effective in the study of the pasta structures. In particular, we showed that topological observables can be used to classify the different structures into recognizable patterns; this allows for cross-model comparison between structures obtained with different approaches and to a quantifiable analysis of the effect the nuclear and Coulomb energy have on the pasta formation and properties. We will study the extent to which the screening length λ affects the morphology of the ground states at zero temperature of nuclear pasta. To this effect, semiclassical molecular dynamic simulations with a screened Coulomb potential and values of λ from 0 to 50 fm were performed. The model used is described in Sec. II, and in Sec. II A numerical aspects of the Coulomb model used are discussed. Topological tools were used to quantitatively analyze that the effect the nuclear and Coulomb energies have on the pasta formation, and its properties are introduced in Sec. II C. Results are presented and discussed in Sec. III.

II. CLASSICAL MOLECULAR DYNAMICS MODEL

The model used here was developed to study nuclear reactions from a semiclassical, particle-based point of view [25]. The justification for using this model in stellar crust environments was presented elsewhere [12]; here we simply mention some basic ingredients of the model.

The classical molecular dynamics model (CMD), as introduced in Ref. [26], is retrofitted with cluster recognition algorithms and a plethora of analysis tools. It has been successfully used in heavy-ion reaction studies to help understand experimental data [27], identify phase-transition signals and other critical phenomena [28–31], and explore the caloric curve [32,33] and isoscaling [34,35]. Synoptically, CMD uses two two-body potentials to describe the motion of nucleons by solving their classical equations of motion. The potentials, developed phenomenologically by Pandharipande [25], are

$$V_{np}(r) = v_r \exp(-\mu_r r)/r - v_a \exp(-\mu_a r)/r,$$
$$V_{nn}(r) = v_0 \exp(-\mu_0 r)/r,$$

where V_{np} is the potential between a neutron and a proton, and V_{nn} is the repulsive interaction between either nn or pp. The cutoff radius is $r_c = 5.4$ fm and for $r > r_c$ both potentials are set to zero. The Yukawa parameters μ_r, μ_a, and μ_0 were determined to yield an equilibrium density of $\rho_0 = 0.16$ fm^{-3}, a binding energy $E(\rho_0) = 16$ MeV/nucleon and a compressibility of 250 MeV [25].

The main advantage of the CMD model is the possibility of knowing the position and momentum of all particles at all times. This allows the study of the structure of the nuclear medium from a particle-wise point of view. The output of CMD; namely, the time evolution of the particles in $(\mathbf{r},\mathbf{p})$, can be used as input in any one of the several cluster-recognition algorithms that some of us have designed for the study of nuclear reactions [36–38].

As explained elsewhere [12,39,40], the lack of quantum effects such as Pauli blocking—perhaps the only serious caveat in classical models—ceases to be relevant in conditions of high density and temperature (such as in heavy-ion reactions) or in the low-density and low-temperature stellar environments, when momentum transfer between particles ceases to be important.

To simulate an infinite medium, systems with thousands of nucleons were constructed using CMD under periodic boundary conditions. Cases symmetric in isospin (i.e., with $x = Z/A = 0.5$, 2500 protons, and 2500 neutrons) were constructed in cubical boxes with sizes adjusted to have densities between $\rho = 0.005$ fm$^{-3} \leqslant \rho \leqslant 0.08$ fm^{-3}. Although in the actual neutron stars the proton fraction is low ($x < 0.5$), we chose to work with symmetric matter because that way we could study the Coulomb term without having a symmetry term in the energy.

A. Coulomb interaction in model

To take into account the Coulomb interaction, which is formally of infinite range, in molecular dynamics simulations with periodic boundary conditions, it is necessary to use some approximation. The two most common approaches are the Thomas–Fermi screened Coulomb potential (used with various nuclear models, e.g., in CMD [12], quantum molecular dynamics [7] and simple semiclassical potential [13]) and the Ewald summation procedure [23]. Theoretical estimations for the screening length λ are $\lambda \sim 100$ fm, but in the previously mentioned works, due to computational limitations, a value of $\lambda = 10$ fm was chosen. Our goal on this work is to understand the effect this *a priori* arbitrary choice has on the properties of the ground states of neutron star matter within the framework of CMD.

In this work, we used values of λ ranging from $\lambda = 0$ fm (formally, no Coulomb interaction) and $\lambda = 20$ fm, for densities $\rho = \{0.005\,\text{fm}^{-3}, 0.03\,\text{fm}^{-3}, 0.05\,\text{fm}^{-3}, 0.08\,\text{fm}^{-3}\}$, and the cutoff length was chosen at $r_c = \lambda$. In particular, for $\rho = 0.005$ fm^{-3}d, where "gnocchi" are formed, we extended the analysis to $\lambda = 30$ fm and $\lambda = 50$ fm to perform a quantitative analysis on the physical properties of the clusters.

B. Simulation procedure

The trajectories of the nucleons are then governed by the Pandharipande and the screened Coulomb potentials. The nuclear system is cooled from $T = 1.6$ MeV to $T = 0.001$ MeV using isothermal molecular dynamics with the Nosé-Hoover thermostat procedure [41], using the LAMMPS package [42]. Systems are cooled in small temperature steps ($\Delta T \approx 0.02$), decreasing the temperature once both the energy and the temperature are stable.

C. Analysis tools

The first of the analysis tools used is the pair correlation function $g(r)$, which gives information about the spatial ordering of the nuclear medium. In the previous study, $g(r)$ showed that nucleons in clusters have an interparticle distance of about 1.8 fm at all studied densities for $\lambda = 10$ fm. It is interesting to know if the nearest-neighbor distance changes with screening length.

TABLE I. Classification breadth: Euler.

	Breadth < 0	Breadth ~ 0	Breadth > 0
Euler > 0	Anti-gnocchi (bubbles)		Gnocchi
Euler ~ 0	Anti-spaghetti (tunnels)	Lasagna	Spaghetti
Euler < 0	Anti-jungle-gym		Jungle gym

Beyond local measures, the shapes of nuclear structures can be characterized by a set of morphological and topological observables: their volume, surface area, mean breadth (area-averaged curvature), and Euler characteristic χ. These four objects comprise the "Minkowski functionals" and completely describe all morphological and topological properties of any three-dimensional object [43]. The computation of the mean breadth and χ can be accomplished through the Michielsen–De-Raed algorithm but requires the mapping of the nuclear clusters into a polyhedra; a procedure described in Ref. [12].

In Ref. [12] it was shown that generic structures, such as gnocchi (droplets), "spaghetti" (rods), "lasagna" (slabs) and "crossed lasagnas" or a set of intertwined rods that resemble Schwartz P surface, that we call "jungle gym" and their inverse structures (with voids replacing particles and vice versa), all have well-defined and distinct values of the mean breadth and χ with magnitudes dictated by the overall size of the structure, i.e., by the number of particles used. For structures with near-zero Euler number, which signal spaghetti, lasagna, and their complementary structures, the values of the Minkowski functionals are sensitive to the choice of two parameters: the size given to each particle and the size of the cells in which we partition the space. This classification is shown in Table I.

III. RESULTS AND DISCUSSION

As observed in previous works [20,21], in absence of any Coulomb interaction (what would be equivalent to $\lambda = 0$), pasta-like structures can be seen, although only one per cell. These *pseudopastas* are also shaped in spheres, rods, slabs, antirods, and antispheres, just like the pasta with Coulomb interactions. The main difference is that, without the Coulomb interaction, we always find one structure per cell, giving the hint that its structure is related to the periodic boundary condition imposed on the box. The *pseudopasta* exists due to finite size effects and, if the box was not to exist, the solution would be an infinite droplet. We notice, however, that when there is Coulomb interaction, the competition between opposing interactions gives rise to a characteristic length. At subsaturation densities, this competition is responsible for the pasta phases, and in the limit of very-low densities (and no screening) it shapes the nuclei we are used to.

By increasing the value of λ, starting from 0 fm, we aim to explore the transition from artificial *one-per-cell* pasta to more realistic situations with more than one structure per cell. Moreover, this enables us to assess the physical implications of the arbitrary and traditional $\lambda = 10$ fm value.

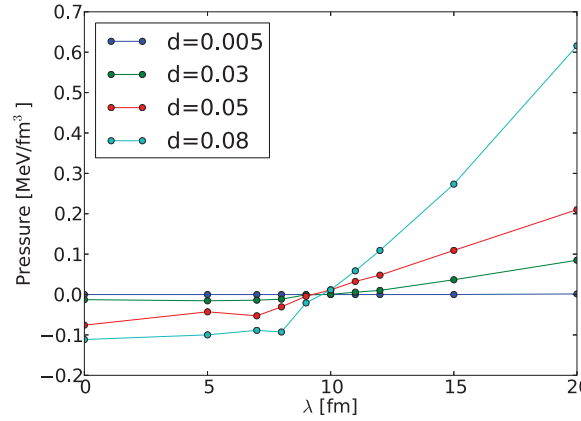

FIG. 1. (Color online) Pressure as a function of λ for different densities. We see that, for $\lambda < 10$ fm, the pressure is negative, implying that periodic boundary conditions are affecting the morphology of the solution.

A. "Critical" screening length

A first approach to analyze the nature of the pasta obtained is given by taking a quick glance as the pressure of the different configurations.

The pressure is computed by the virial formula

$$P = \frac{N k_B T}{V} + \frac{1}{3}\frac{\Sigma_i^N \mathbf{r}_i \cdot \mathbf{F}_i}{V},$$

where N is the number of nucleons in the system and $\mathbf{F}$ is the force exerted upon each nucleon. The terms in the virial formula apply only to the interactions specific to the model, not contemplating the electron-gas pressure. This pressure is not to be mistaken with the pressure expected in neutron star crusts (since electrons should be considered explicitly in order to calculate it correctly); it is merely a test of the mechanical stability of the configurations obtained within this model. In Fig. 1, we see that for all $\lambda < 10$ fm the pressure is negative.

The negative pressure is a signal that the nonhomogeneous structures found are artificial and that the structures found can only exist under periodic boundary conditions (see Refs. [20,22]). This may be better understood by picturing the primitive cell of the simulation as being under the stress caused by its periodic replicas. This means that for such small screening lengths the overall effective interaction is mostly attractive and periodic boundary conditions are still playing a major role in shaping the ground state.

For $\lambda > 10$ fm the pressure becomes positive, meaning that the structures formed in these configurations are not only due to periodic boundary conditions, but the Coulomb interaction is beginning to play its intended role. The configurations for these values of λ indeed show density fluctuations of length smaller than the size of the cell, which can only be attributed to the Coulomb-nuclear competition. However, the morphology of the structures, as characterized by the topological measures described in Sec. II C, changes drastically with λ.

In order to classify the low temperature ($T = 0.001$ MeV) structures for each value of λ, we study their morphology with the analysis tools for the spatial distribution of the particles;

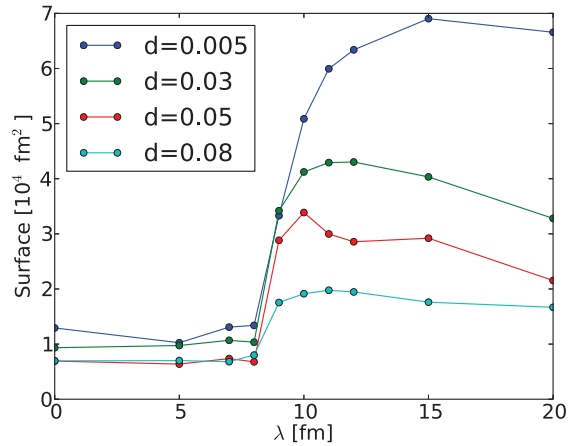

(a) Surface

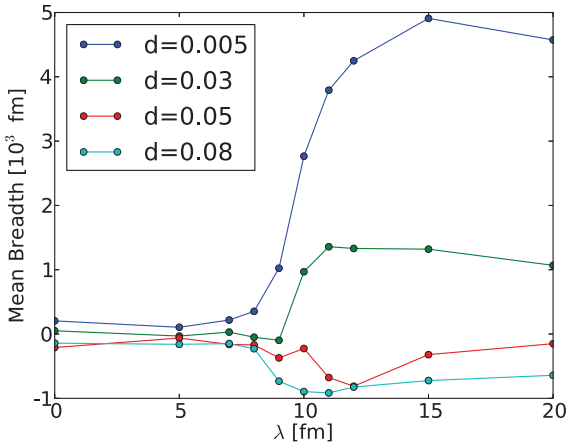

(b) Mean Breadth

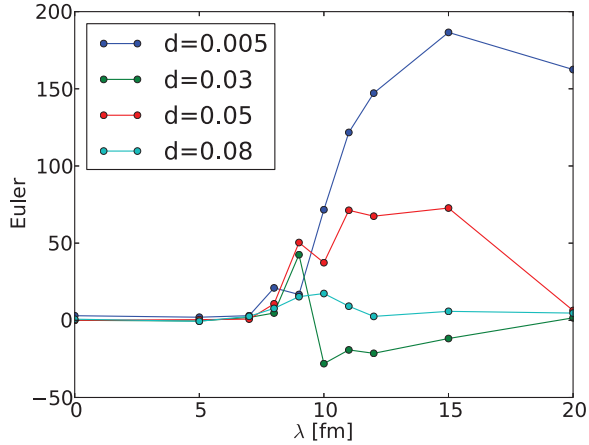

(c) Euler number

FIG. 2. (Color online) Minkowski functionals dependence on λ. We can see that there is a transition regime between λ = 7 fm and λ = 15 fm where the Minkowski functionals are changing.

namely, the Minkowski functionals. In Fig. 2 we can see the surface, mean breadth, and Euler number for the ground states, and their dependence on λ for different densities.

As stated in Table I, we expect *lasagna* and *spaghetti* to have an Euler number $\chi = 0$. In the *gnocchi* case, however, each one of them contributes with $\chi_{gn} = 2$. This means that the Euler number for the whole system of N_{gn} *gnocchi* will be $\chi = 2N_{gn}$. As the configurations break up into multiple structures per cell with increasing λ, we expect the surface to increase as well. As for the mean breadth, the behavior described in Table I (positive for *spaghetti* and *gnocchi*, zero for *lasagna*, and negative for *tunnel*) is only observed for λ = 20 fm. Between λ = 7 fm and λ = 10 fm all three of the Minkowski functionals change drastically before reaching well-defined values. This indicates that there is a transition regime where the structures cannot be described as any of the traditional pasta. For this model of nuclear interaction and Coulomb treatment, it seems the usual λ = 10 fm value is actually too small.

B. One vs many

To better understand how the ground state at low temperatures varies through the transition regime from without Coulomb interaction to the λ = 20 fm screening length, we show in Fig. 3 visual representations of the results obtained at a set of chosen densities, with λ = 0, λ = 10 fm, and λ = 20 fm. We see here that we get very exotic and amorphous structures for λ = 10 fm in all three cases, and they are variations from the typical pasta structure, which can be due to the very rough energy landscape for this values of λ.

As an example, we show the pair distribution function $g(r)$ for $\rho = 0.05$ fm^{-3} in Fig. 4. In it we see that the first peaks of the distribution remain at the same distances of $r = 1.7$ fm, 1.9 fm. This shows that the short-range structure is governed by the nuclear potential even at λ = 20 fm, which is evident simply by comparing the orders of magnitude of V_{n-n} and V_{Coulomb} at such short ranges.

At density $\rho = 0.005$ fm^{-3}, for screening lengths λ < 10 fm, there is a single *gnocchi*. However, when increasing from λ = 15 fm to λ = 20 fm at $\rho = 0.005$ fm^{-3}, although qualitatively we see the same behavior (both show *gnocchi*), the average size of clusters is different for these two values of screening length. This implies that the number of clusters is different; hence the difference observed in the Minkowski functionals. To study this result further, we plot the gnocchi size as a function of λ in Fig. 5. We see that, when we consider the standard deviation in the mass distribution, it remains unchanged for λ ⩾ 20 fm. The average relative error on this graph is $e \approx 8\%$.

We can see here, however, that although every structure without the Coulomb interaction is indeed one of the known pasta structures, once we turn on the Coulomb interaction (by making λ ≠ 0) the original λ = 0 *pseudopasta* splits up: from one structure per cell to multiple structures per cell. For intermediate to low values of λ < 20 fm, the effect of the periodic boundary conditions is still observable for some densities, and more exotic structures which can be confused with "true" pasta may exist.

C. Transition regime

We now turn to analyze the structures found in the transition regime.

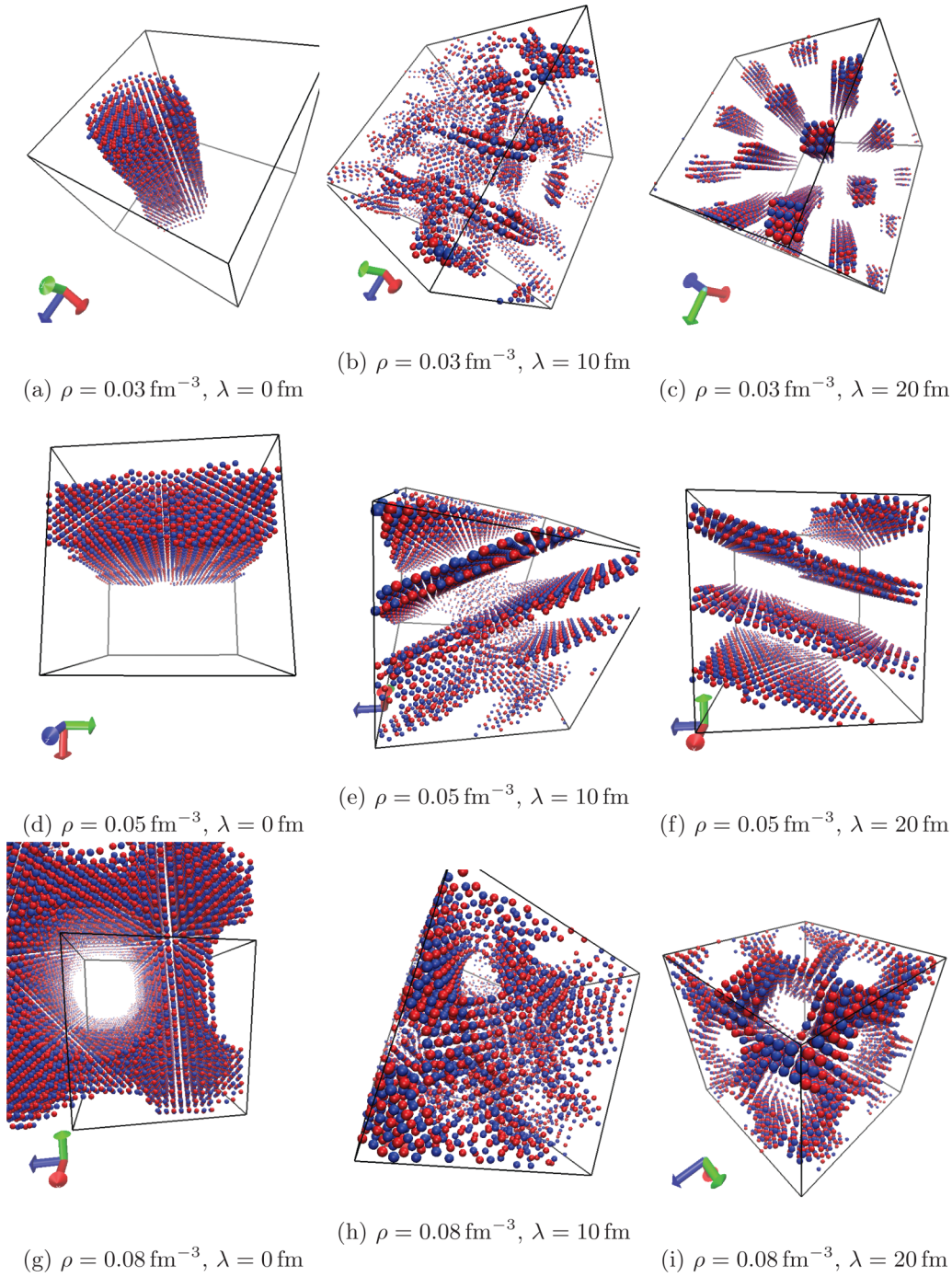

(a) $\rho = 0.03\,\mathrm{fm}^{-3}$, $\lambda = 0\,\mathrm{fm}$ (b) $\rho = 0.03\,\mathrm{fm}^{-3}$, $\lambda = 10\,\mathrm{fm}$ (c) $\rho = 0.03\,\mathrm{fm}^{-3}$, $\lambda = 20\,\mathrm{fm}$

(d) $\rho = 0.05\,\mathrm{fm}^{-3}$, $\lambda = 0\,\mathrm{fm}$ (e) $\rho = 0.05\,\mathrm{fm}^{-3}$, $\lambda = 10\,\mathrm{fm}$ (f) $\rho = 0.05\,\mathrm{fm}^{-3}$, $\lambda = 20\,\mathrm{fm}$

(g) $\rho = 0.08\,\mathrm{fm}^{-3}$, $\lambda = 0\,\mathrm{fm}$ (h) $\rho = 0.08\,\mathrm{fm}^{-3}$, $\lambda = 10\,\mathrm{fm}$ (i) $\rho = 0.08\,\mathrm{fm}^{-3}$, $\lambda = 20\,\mathrm{fm}$

FIG. 3. (Color online) Difference between pasta with and without the Coulomb interaction. We can see that the Coulomb interaction splits up the pasta, converting one structure per cell to multiple structures per cell.

We take, as an example, the lowest density ($\rho = 0.005$ fm^{-3}). As can be seen in Fig. 6, for $\lambda = 0$ only one droplet is formed, as expected. For $\lambda = 10$ fm, we can see that many *gnocchi* exist, but some of them stick to their neighbors forming prolates of different sizes. Although the Coulomb interaction is now strong enough to break the one pasta found with $\lambda = 0$ into many, the resulting droplets are not fully fledged gnocchi that can be arranged in a regular lattice such as those found for $\lambda = 20$ fm.

IV. DISCUSSION AND CONCLUDING REMARKS

The effect of the screening length of the Coulomb interaction in simulations of neutron star matter was studied at densities comparable to that of neutron stars crusts. Throughout the literature we can find that the value of the screening length in the Thomas–Fermi approximation is $\lambda \approx 100$ fm. For particle-based simulations, due to computational limitations, this value was historically and arbitrarily reduced to $\lambda \approx 10$ fm. This was done expecting to maintain the basic phenomenology when

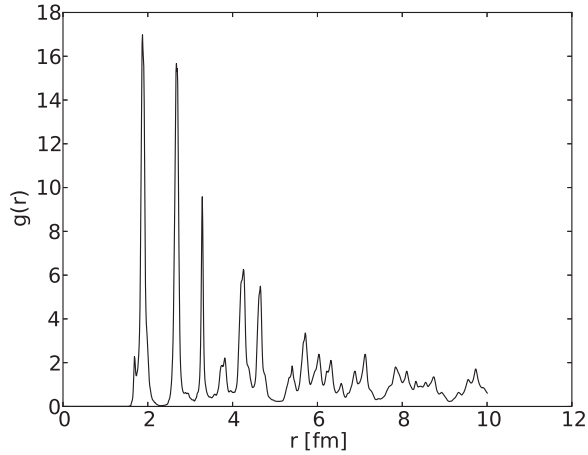

(a) Multiple lasagna

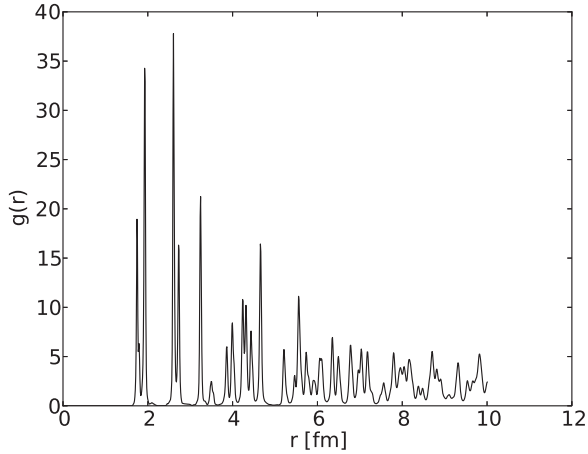

(b) Single lasagna

FIG. 4. Examples of the radial correlation function for $\rho = 0.05$ fm^{-3} and two screening lengths: $\lambda = 20$ fm (top panel) and $\lambda = 0$ fm (lower panel). Please notice the difference in the y scales of the graphs.

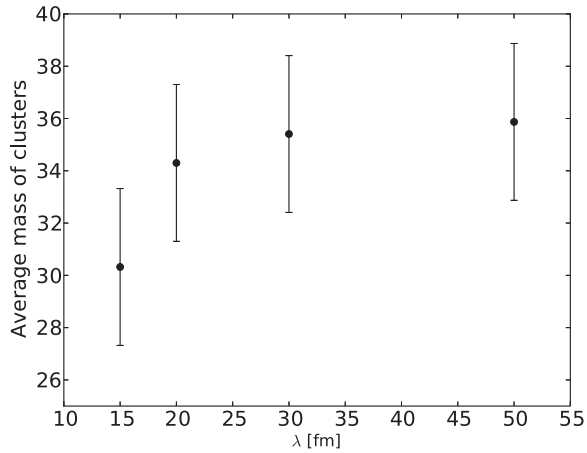

FIG. 5. Average size of nuclei depending on screening length. We can see that, when considering the standard deviation, the mass remains the same.

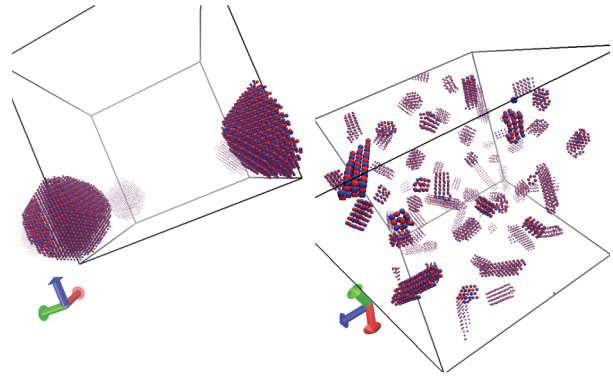

(a) $\lambda = 0$ fm (b) $\lambda = 10$ fm

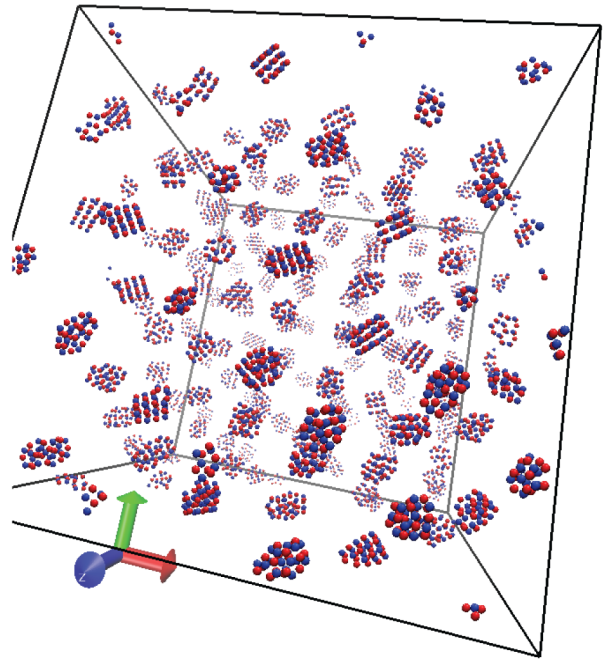

(c) $\lambda = 20$ fm

FIG. 6. (Color online) Different structures obtained while varying the λ parameter for $\rho = 0.005$ fm^{-3}. In the transition regime, we find, at $\lambda = 10$ fm, that the structure breaks down to many *short-spaghetti*-like parts.

simulating small systems. We found, though, that there is a critical screening length λ_c at which the structure of the ground state drastically changes. For the Pandharipande potential it lies between 10 and 15 fm (depending on the density). For $\lambda < \lambda_c$, the Coulomb interaction is barely acting and the nonhomogeneous structures emerging from the simulations are due to finite-size effects, as made evident from the negative pressure of such structures and the fact that there is only one structure per cell. For $\lambda > \lambda_c$, the pressure becomes positive and the systems present density fluctuations at a scale smaller than that of the cell, but not well shaped. This transition regime is characterized by large fluctuations in the surface, mean breadth, and Euler characteristic χ of the structures. It is only for $\lambda = 20$ fm that the morphology of the structures formed

stabilizes and ceases to depend on λ. Moreover, the structures in this regime are the usual pasta phases.

Because of this, we believe extreme caution should be taken when choosing an arbitrary value for λ, since even though some results at $\lambda = 10$ fm can look like the expected pasta, the results obtained for that particular choice of λ may be quite different from those in the true Thomas–Fermi approximation. In conclusion, we find the choice of a good value for λ that is computationally manageable and can still adequately recover the physics of the Thomas–Fermi approximation is no trivial task, and a rigorous study needs to be done prior to the choice of the value. A good value for λ must lie in the $\lambda > \lambda_c$ region which is bound to be dependent on the model used for the nuclear interaction.

ACKNOWLEDGMENTS

C.O.D. is supported by CONICET Grant PIP0871; P.G.M., J.I.N., and P.N.A. are supported by a CONICET grant. The three-dimensional figures were prepared using the software VISUAL MOLECULAR DYNAMICS [44].

[1] D. G. Ravenhall, C. J. Pethick, and J. R. Wilson, Phys. Rev. Lett. **50**, 2066 (1983).
[2] M. Hashimoto, H. Seki, and M. Yamada, Prog. Theor. Phys. **71**, 320 (1984).
[3] R. D. Williams and S. E. Koonin, Nucl. Phys. A **435**, 844 (1985).
[4] K. Oyamatsu, Nucl. Phys. A **561**, 431 (1993).
[5] C. P. Lorenz, D. G. Ravenhall, and C. J. Pethick, Phys. Rev. Lett. **70**, 379 (1993).
[6] K. S. Cheng, C. C. Yao, and Z. G. Dai, Phys. Rev. C **55**, 2092 (1997).
[7] T. Maruyama, K. Niita, K. Oyamatsu, T. Maruyama, S. Chiba, and A. Iwamoto, Phys. Rev. C **57**, 655 (1998).
[8] T. Kido, Toshiki Maruyama, K. Niita, and S. Chiba, Nucl. Phys. A **663-664**, 877c (2000).
[9] G. Watanabe, K. Iida, and K. Sato, Nucl. Phys. A **676**, 455 (2000).
[10] G. Watanabe, K. Sato, K. Yasuoka, and T. Ebisuzaki, Phys. Rev. C **66**, 012801 (2002).
[11] G. Watanabe and K. Iida, Phys. Rev. C **68**, 045801 (2003).
[12] C. O. Dorso, P. A. Giménez Molinelli, and J. A. López, in *Neutron Star Crust*, edited by C. A. Bertulani and J. Piekarewicz (Nova Science Publishers, Inc., New York, 2012).
[13] C. J. Horowitz, M. A. Perez-Garcia, and J. Piekarewicz, Phys. Rev. C **69**, 045804 (2004).
[14] Y. Mochizuki and T. Izuyama, Astrophys. J. **440**, 263 (1995).
[15] A. L. Fetter and J. D. Wallecka, *Quantum Theory of Many-Particle Systems* (McGraw-Hill, San Francisco, 1971).
[16] D. Frenkel and B. Smit, *Understanding Molecular Simulations*, 2nd ed. (Academic Press, New York, 2002).
[17] T. Maruyama, G. Watanabe, and S. Chiba, Prog. Theor. Exp. Phys. **2012**, 01A201 (2012).
[18] T. Maruyama, T. Tatsumi, D. N. Voskresensky, T. Tanigawa, and S. Chiba, Phys. Rev. C **72**, 015802 (2005).
[19] G. Watanabe, AIP Conf. Proc. **891**, 373 (2007).
[20] C. O. Dorso, P. A. Giménez Molinelli, J. I. Nichols, and J. A. López, Nucl. Phys. A **923**, 31 (2014).
[21] A. S. Schneider, C. J. Horowitz, J. Hughto, and D. K. Berry, Phys. Rev. C **88**, 065807 (2013).
[22] K. Binder *et al.*, Am. J. Phys. **80**, 1099 (2012).
[23] G. Watanabe, K. Sato, K. Yasuoka, and T. Ebisuzaki, Phys. Rev. C **68**, 035806 (2003).
[24] H. Sonoda, G. Watanabe, K. Sato, K. Yasuoka, and T. Ebisuzaki, Phys. Rev. C **77**, 035806 (2008).
[25] A. Vicentini, G. Jacucci, and V. R. Pandharipande, Phys. Rev. C **31**, 1783 (1985); R. J. Lenk and V. R. Pandharipande, *ibid.* **34**, 177 (1986); R. J. Lenk, T. J. Schlagel, and V. R. Pandharipande, *ibid.* **42**, 372 (1990).
[26] A. Barrañón, C. O. Dorso, J. A. López, and J. Morales, Rev. Mex. Fís. **45**, 110 (1999).
[27] A. Chernomoretz, L. Gingras, Y. Larochelle, L. Beaulieu, R. Roy, C. St-Pierre, and C. O. Dorso, Phys. Rev. C **65**, 054613 (2002).
[28] A. Barrañón, C. O. Dorso, and J. A. López, Rev. Mex. Fís. **47**, 93 (2001).
[29] A. Barrañón, C. O. Dorso, and J. A. López, Nucl. Phys. A **791**, 222 (2007).
[30] A. Barrañón, R. Cárdenas, C. O. Dorso, and J. A. López, Acta Phys. Hung. New Ser.: Heavy Ion Phys. **17**, 59 (2003).
[31] C. O. Dorso and J. A. López, Phys. Rev. C **64**, 027602 (2001).
[32] A. Barrañón, J. Escamilla Roa, and J. A. López, Braz. J. Phys. **34**, 904 (2004).
[33] A. Barrañón, J. Escamilla Roa, and J. A. López, Phys. Rev. C **69**, 014601 (2004).
[34] C. O. Dorso, C. R. Escudero, M. Ison, and J. A. López, Phys. Rev. C **73**, 044601 (2006).
[35] C. O. Dorso, P. A. Giménez Molinelli, and J. A. López, J. Phys. G **38**, 115101 (2011); Rev. Mex. Fís. **57**, 14 (2011).
[36] C. O. Dorso and J. Aichelin, Phys. Lett. B **345**, 197 (1995).
[37] A. Strachan and C. O. Dorso, Phys. Rev. C **55**, 775 (1997); **56**, 995 (1997).
[38] C. O. Dorso and J. Randrup, Phys. Lett. B **301**, 328 (1993).
[39] J. A. López and C. O. Dorso, *Lecture Notes on Phase Transformations in Nuclear Matter* (World Scientific, Hackensack, 2000).
[40] J. Taruna, Ph.D. thesis, Florida State University, 2008.
[41] S. Nose, J. Chem. Phys. **81**, 511 (1984).
[42] S. Plimpton, J. Comput. Phys. **117**, 1 (1995).
[43] K. Michielsen and H. De Raedt, Phys. Rep. **347**, 461 (2001).
[44] W. Humphrey, A. Dalke, and K. Schulten, J. Mol. Graphics **14**, 33 (1996).